

ELECTROMIGRATION INTERCONNECT LIFETIME UNDER AC AND PULSE DC STRESS

B. K. Liew, N. W. Cheung, and C. Hu

Department of Electrical Engineering and Computer Sciences,
University of California, Berkeley, California 94720
(415) 643-7036

Abstract

We propose a vacancy relaxation model which predicts that DC lifetime is $A_{DC}(T) / J^m$, pulse DC lifetime is $A_{DC}(T) / \bar{J} J^{m-1}$, and AC lifetime is $A_{AC}(T) / |J| |J|^{m-1}$ for all waveforms and all frequencies above 10kHz. The AC lifetimes of aluminum interconnect are experimentally found to be more than 10^3 times larger than DC lifetime at the same current density. (AC stress lifetimes have the same dependences on current magnitude and temperature, for $T < 300^\circ\text{C}$, as the DC stress lifetime.)

Introduction

The electromigration failure of Al interconnect has been extensively studied under constant current conditions. Integrated circuits, however, often operate with time-varying uni-directional (pulse DC) or bi-directional (AC) current waveforms. For the case of uni-directional currents (which are found in the power bus lines), the assumption is often made that the conductor lifetime increases linearly with the reciprocal of the duty factor (i.e., the total on-time to failure is the same in constant DC and pulse DC experiments). However, our experimental results, as well as others [1-4] indicate considerably larger pulse DC lifetime than predicted by this simple model. As for the case of AC conditions (which is found in signal lines of NMOS and CMOS circuits), the proper method of predicting lifetime becomes even less obvious because the direction of current is time varying and so is the flux of Al atoms in the interconnect. The question is often asked whether electromigration lifetime under AC current is very long because of the reversible flow of atomic flux, or is not very different from the DC stress lifetime. We present a theoretical model that predicts the correlations among the lifetimes under these conditions and the constant current stress lifetime, which can be measured easily. The objective of our work is to apply this model to predict pulse DC and AC lifetimes under arbitrary current waveforms and frequencies using constant DC stressing results, or minimum amount of additional test results.

Model

Figure 1 illustrates the general model [5]. Let δ be the volume of the void (or some other measure of the damage which eventually leads to failure) in the interconnect. The rate of increase of δ should be proportional to the vacancy flux, F_v , which is equal to the product of vacancy concentration n and vacancy velocity v . The velocity has been shown to be proportional to the current density J , independent of pulse duty factor (0.02 - 0.9) and frequency (0.01 - 10^5 Hz) in pulse DC experiment [1]. The time derivative of δ can be written as:

$$\frac{d\delta}{dt} \propto F_v = nv \propto nJ \quad (1)$$

$$= R(\delta) n(t) J(t) \quad (2)$$

The proportionality constant R is allowed to be a function of δ , i.e. varying during the stress, for generality. The time-to-failure, TTF is the time required for δ to reach some critical value δ_c :

$$\int_0^{\text{TTF}} n(t) J(t) dt = \int_0^{\delta_c} \frac{d\delta}{R(\delta)} \equiv K \quad (3)$$

One may define TTF as the median time-to-failure (MTF) or 1% population failure time or any other failure time. Assuming that the vacancy relaxation time is τ and the vacancy generation rate is proportional to $|J|^{m-1}$ (the use of exponent $m-1$ will be justified later) with a proportionality constant α .

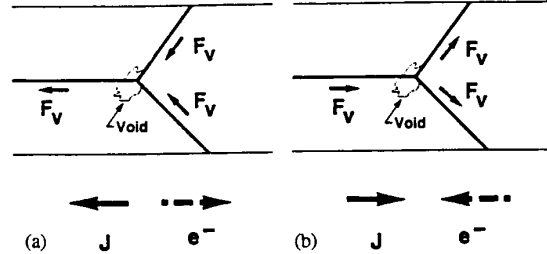


Fig.1. (a) In DC and pulse DC cases, the volume of the void, δ , increases with time at a rate proportional to the product of vacancy concentration n and velocity v . In pure AC case, the volume of void grows during the first half cycle in (a) and decreases in (b) during the opposite current period. As a result, the proportionality constants R_+ and R_- in Eqs.(12) are different.

$$\frac{dn}{dt} = -\frac{n}{\tau} + \alpha |J(t)|^{m-1} \quad (4)$$

The absolute sign is used here because the number of vacancies generated depends on the number of electrons available for momentum transfer to the lattice and does not depend on the direction of electron flow. For a given waveform $J(t)$, one can solve Eq.(4) for $n(t)$ and substitute $n(t)$ into Eq.(3) to find the TTF.

DC case: Using Eq.(3) and (4):

$$n = \tau \alpha J_{DC}^{m-1} \quad (5)$$

$$\text{TTF}_{DC} = \frac{K}{\tau \alpha J_{DC}^m} \quad (6)$$

By observation, $K/\tau\alpha$ is simply equal to the $A_{DC}(T)$ in the Black's equation:

$$\text{TTF}_{DC} = \frac{A_{DC}(T)}{J_{DC}^m} \quad (7)$$

The reason for choosing the functional form of vacancy generation rate as J^{m-1} is now obvious.

Pulse DC case: The vacancy relaxation time τ is about 1ms [6]. For all frequencies much higher than $1/\tau$, i.e. above 10 kHz, $n(t)$ reaches steady state value after a few τ 's and consists of a small ripple superimposed on an average, \bar{n} . \bar{n} can be obtained by taking the time average of every term in Eq.(4) and realizing that L.H.S. of Eq.(4) integrated over one period is zero:

$$n(t) \approx \bar{n} = \tau \alpha \bar{J}^{m-1} \quad (8)$$

The total time to failure which includes the on-time and off-time of the waveform is:

$$\begin{aligned} \text{TTF}_{\text{pulse DC}} &= \frac{K}{\tau \alpha \bar{J} J^{m-1}} \\ &= \frac{A_{DC}(T)}{\bar{J} J^{m-1}} \end{aligned} \quad (9)$$

where $A_{DC}(T)$ is the same as that obtained from DC measurement (Eq.(7)). For the special case of rectangular DC pulses, $TTF_{pulse\ DC}$ can be related to TTF_{DC} (with $J_{DC} = J_{peak}$) for all exponent values, m , except for $m=1$ by:

$$TTF_{pulse\ DC} = TTF_{DC}(\text{Duty Factor})^{-2} \quad (10)$$

For the case of $m=1$ and $m=2$, Eq.(9) becomes

$$TTF = \frac{A_{DC}(T)}{\bar{J}^m} \quad (11)$$

Pure AC case:

The time derivative of δ can be written as:

$$\frac{d\delta}{dt} = R_+(\delta) n(t) |J(t)|$$

during the positive cycle and

$$= -R_-(\delta) n(t) |J(t)| \quad (12)$$

during the negative cycle. At any given δ , the values and the signs of $R_+(\delta)$ and $R_-(\delta)$ are in general not the same. The non-symmetrical flow of vacancy flux due to the geometry of the interconnect (e.g. near the bond pads) or at grain boundary triple point can give rise to different values of R_- and R_+ . The latter effect can be inferred from Fig.1. The negative sign in front of R_- represents the probable existence of healing effect by current of opposite polarities. However, R_- can take on a negative sign if the void is enlarged by current of both polarities. Therefore, Eqs.(12) are quite general.

The vacancy generation rate is independent of the sign of current density. Taking the time average of Eq.(4) yields:

$$n(t) = \bar{n}_{AC} = \tau \alpha |J|^{m-1} \quad (13)$$

Summing the damage in one period, Δt , using Eq.(11):

$$\frac{\Delta\delta}{\Delta t} = \frac{[R_+(\delta) - R_-(\delta)]}{2} \alpha |J| |J|^{m-1} \quad (14)$$

The factor of half comes from the fact that for pure AC waveform, the time integral of the current density over the positive cycle is equal to the integral over the negative cycle, and is equal to one half the time average of $|J|$ in one period. Following the procedure of Eq.(3):

$$\begin{aligned} TTF_{AC} &= \frac{2}{\tau \alpha |J| |J|^{m-1}} \int_0^{\delta_c} \frac{d\delta}{R_+(\delta) - R_-(\delta)} \\ &\equiv \frac{A_{AC}(T)}{|J| |J|^{m-1}} \end{aligned} \quad (15)$$

Please note the $A_{AC}(T)$ has no direct correlation with $A_{DC}(T)$. Therefore, at least one AC test using a convenient waveform and frequency, e.g. 10kHz square wave, needs to be carried out in order to determine $A_{AC}(T)$. Subsequently, Eq.(15) can be used to predict TTF_{AC} for other current waveforms, magnitudes and frequencies.

Experimental Design

Al-2%Si film of 800Å thickness was sputter-deposited in CPA 9900 sputtering system onto patterned silicon wafers covered with 400Å SiO₂. The small thicknesses were chosen to minimize heat dissipation and thermal resistance of the test lines. A lift-off process was used to fabricate groups of 1.2 and 2.2 μm wide, 100, 800 and 1600 μm long test stripes. Prior to electrical testing, the wafers were annealed at 400°C for 20 minutes in forming gas. The sheet resistance of the film was 360 mΩ per square. The test structures were unpassivated. Testing was performed by placing the wafers on the heated stage of a probe station. Current was passed through the test stripes from micromanipulator probes.

Pulse DC and AC currents were generated from a transistor current source driven by the output a TTL gate (Fig.2). The setup had six current sources to stress six stripes simultaneously. The output impedance of the current source is large enough to ensure that variation in the stripe resistance would have no effect on the stress current. Prior to testing, the temperature coefficient of Al line resistance was obtained in order

to determine the temperature rise due to self-heating of the test stripes under current stressing. During stress, Keithley 196 DMM was used to measure resistance of the test stripes without interrupting the current stressing in spite of the time varying stress current in the test stripe. This was possible by using the compensated mode of the DMM and the fact that the instrument has low bandwidth. Open failure was used as the failure criterion in our testing. MTF of each test condition was found by assuming a log normal failure distribution, and was adjusted for stripe temperature once the activation energy was determined.

Rectangular pulse DC and AC current waveforms of peak current densities from $1 \times 10^7 A/cm^2$ to $6 \times 10^7 A/cm^2$ in the frequencies range of 30kHz to 25MHz were used in this work. The current waveform imposed through any of the test stripes could be monitored with an oscilloscope. An example of the ac waveform is shown in Fig.3.

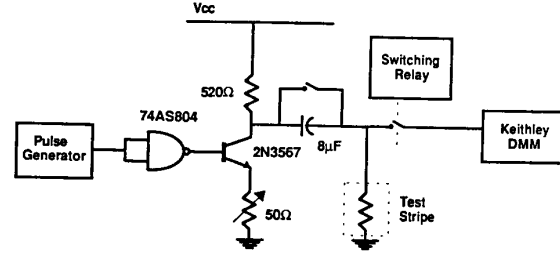


Fig.2. DC, pulse DC and pure AC current stressing circuit. The transistor is switched off during DC stressing and the capacitor is bypassed. For pulse DC stressing, only the capacitor is bypassed. Resistance measurement of six test stripes is done through a switching relay.

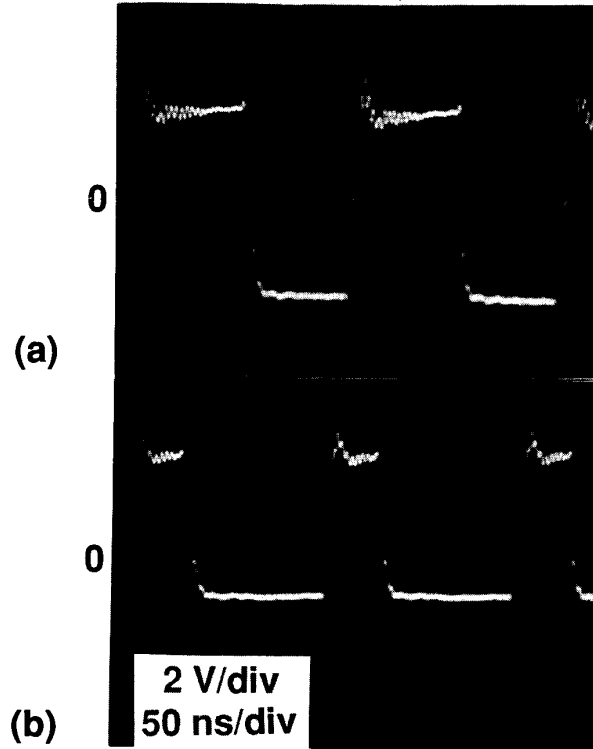


Fig.3. Examples of pure AC waveforms used in this work: (a) symmetrical ($J_+ = J_-$) and (b) non-symmetrical ($J_+ \neq J_-$) waveforms.

Results and Discussion

Pulse DC:

The effect of duty factor on MTF for stripes stressed by rectangular current pulses at frequency of 2.5MHz is shown in Fig.4. Although the peak current density of the pulse was $1 \times 10^7 A/cm^2$, there is minimal self-heating in these tests, i.e. less than $10C^\circ$ for dc current (100% duty factor). Included in Fig.4 are pulse dc results from various authors [2-4]. Their data and ours, fit the following relationship with duty factor:

$$MTF_{\text{pulse DC}} = MTF_{\text{DC}} (\text{Duty Factor})^{-2} \quad (16)$$

This is in agreement with Eq.(10) for the special case of rectangular DC.

Eq.(9) suggests that if $m=2$, $MTF_{\text{pulse DC}}$ can simply be calculated by substituting the time-averaged current density \bar{J} in the Black's equation (Eq.(7)).

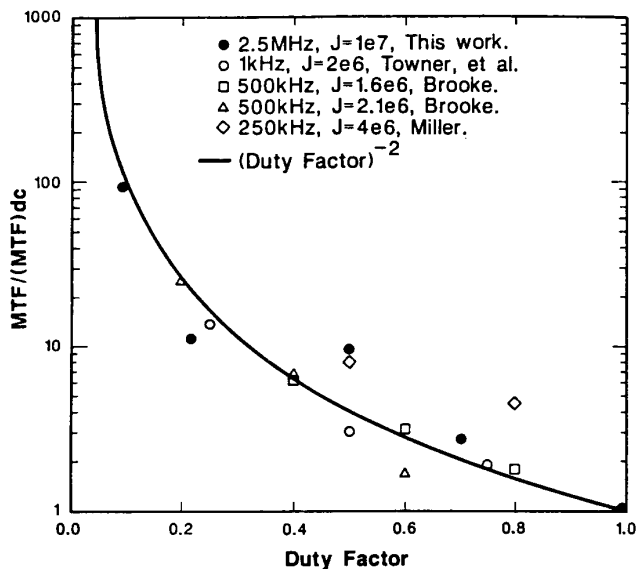


Fig.4. Comparison of our pulse DC MTF results and others' [2-4] with $1/(\text{Duty Factor})^2$. The current densities indicated in the legend are peak current densities. The test stripes used in our work were $1600 \mu\text{m}$ long, $2.2 \mu\text{m}$ wide and $0.08 \mu\text{m}$ thick.

Pure AC:

Our preliminary AC result shows that AC lifetime is 10^4 larger than DC lifetime for the $800 \mu\text{m}$ long stripes stressed with peak current density of $1 \times 10^7 A/cm^2$ (Fig.5). The failure sites of all six stripes were located near the middle of the stripe (Fig.6).

AC MTF obtained from full duty, symmetrical rectangular waveforms (i.e. equal widths and heights in positive and negative halves of the waveform) of various frequencies is plotted against current densities in Fig.7. In order to obtain AC lifetime results in reasonable length of time, we used peak current densities from $2 \times 10^7 A/cm^2$ to $6 \times 10^7 A/cm^2$ with $100 \mu\text{m}$ long $1.2 \mu\text{m}$ wide and 800 \AA thick stripes in all AC testing. For comparison, the DC MTF for the same stripes is included in Fig.7. The data plotted in Fig.7 were corrected for the actual stripe temperature and normalized to 250°C using measured AC and DC MTF activation energies. The value of m , in the exponent of current density in Eq.(15) for AC and DC MTF is found to be 7.5. The high values of m compared to the usual value of 2, may be attributed to the large current densities used in our experiment. Similar large values of m have been reported in other DC stress studies where high current densities were used [7-9]. The equally high value of m for DC MTF results verifies

that large m is not a result of AC stressing. This observation justifies the use of the same m for both AC and DC lifetime prediction in our model. The ratio of $MTF_{\text{AC}}/MTF_{\text{DC}}$ versus current densities for stripe temperature $T=250^\circ\text{C}$ is typically 1000 independent of J as shown in Fig.7. In other words, the A_{AC} term in Eq.(15) is much larger than the usually measured A_{DC} term in Eq.(7). Theoretically this suggests that $R_+(\delta)-R_-(\delta)$ in Eq.(15) is much smaller than R in Eq.(2), which we expect to be comparable to R_+ and R_- .

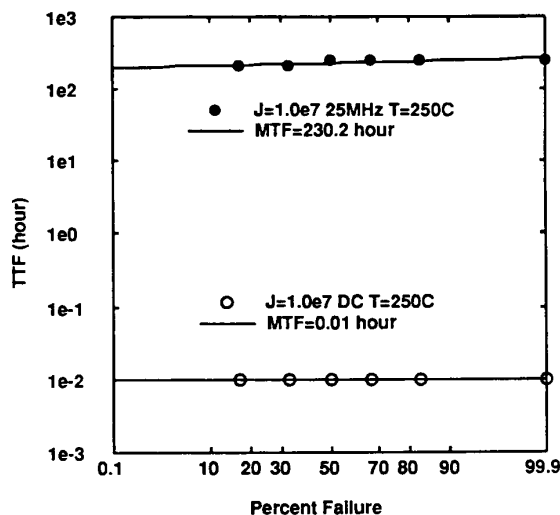


Fig.5. DC and AC lifetimes for $800 \mu\text{m}$ long, $1.2 \mu\text{m}$ wide and $0.08 \mu\text{m}$ thick Al-2%Si stressed at $J=1.0 \times 10^7 A/cm^2$, $T=250^\circ\text{C}$.

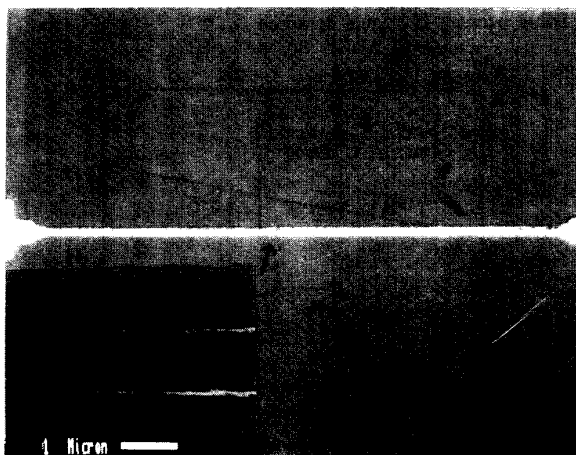


Fig.6. Photograph of failure site for $800 \mu\text{m}$ long, $1.2 \mu\text{m}$ wide and $0.08 \mu\text{m}$ thick stripe stressed using pure AC current and a scanning electron micrograph of the failure site in the inset, $J=1.0 \times 10^7 A/cm^2$, 25MHz, $T=250^\circ\text{C}$.

The activation energy of AC stress lifetime was found from constant current stressing at several wafer chuck temperatures and two peak current densities of $3.3 \times 10^7 A/cm^2$ and $5.0 \times 10^7 A/cm^2$ (Fig.8). Self-heating of the stripes at these two current densities raised stripe temperatures by 60°C and 140°C respectively. The activation energy found from the DC and AC MTF data was 0.33eV . At temperatures larger than 300°C , the AC MTF data display a sharper reduction (Fig.8). Possibly, a second temperature activated process is responsible for this effect. This process is not observed in the uni-directional electromigration experiment because it is much weaker than the usual kinetics (which has $E_a=0.33\text{eV}$) in DC experiment. How-

ever, in bi-directional (AC) electromigration experiment, the net rate of the $E_a=0.33eV$ process, due to the $R_+(\delta)-R_-(\delta)$ term in Eq.(15), is greatly reduced by the healing effect so that the other mechanism becomes observable or, this mechanism may arise from the asymmetry in the process of sinking vacancies into and the process of removing vacancies from the void.

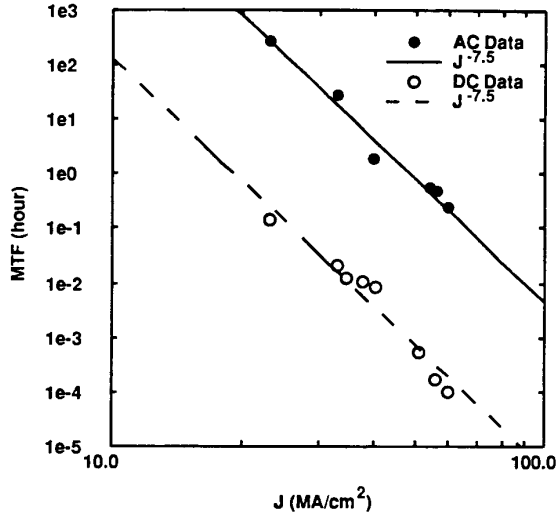


Fig.7. The DC and AC MTF for 100 μm long, 1.2 μm wide and 0.08 μm thick Al-2%Si as a function of current densities. The data have been corrected for self-heating and normalized to $T=250^\circ\text{C}$. Both sets of data fit well with $J^{-7.5}$. The ratio of MTF_{AC} and MTF_{DC} is about 1000 and is independent of current densities.

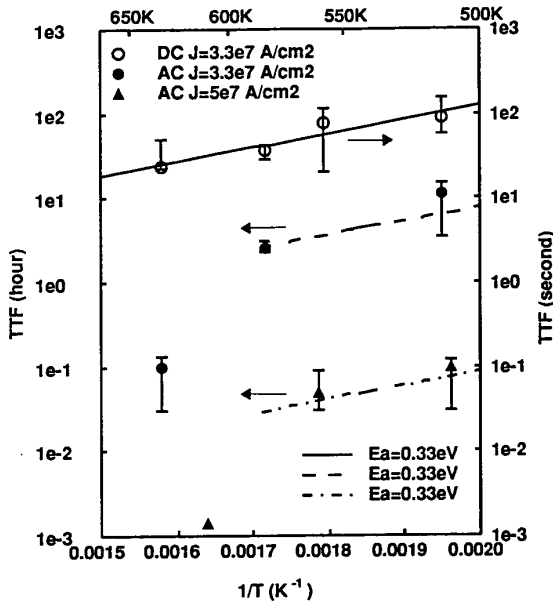


Fig.8. Arrhenius plot of AC and DC MTF. The extracted activation energy for DC and AC MTF is 0.33eV.

In addition to using symmetrical AC ($J_+=J_-$) waveforms in our experiment, we attempted several non-symmetrical but pure AC (no DC component of current) rectangular waveforms (for example, see Fig.3(b.)) and the MTF_{AC} of test stripes stressed with these waveforms is plotted against $|J_+||J_-|^{m-1}$ using $m=7.5$ in Fig.9. The results demonstrate the applicability of Eq.(15) to non-symmetrical pure AC waveforms. The MTF_{AC} for the non-symmetrical waveforms are about 3 times lower than predicted by Eq.(15), which we speculate is due to a weak dependence of R_+ and R_- on current density. The values of $A_{\text{AC}}(T)$ were plotted against the frequencies of the AC current in Fig.10. $A_{\text{AC}}(T)$ is found by multiplying MTF_{AC} with $|J_+||J_-|^{m-1}$ (Eq.(15)) using $m=7.5$. Our model predicts that AC lifetime is insensitive to frequency, which is in agreement with the data plotted in Fig.10. in the range from 35kHz to 14MHz.

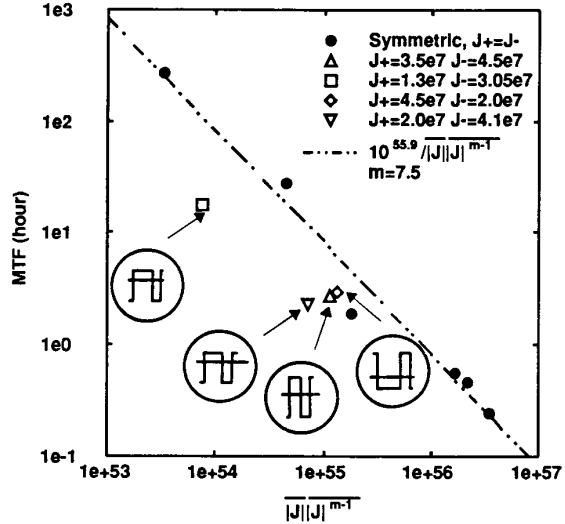


Fig.9. AC MTF plotted against $|J_+||J_-|^{m-1}$ for symmetrical and non-symmetrical AC waveforms (indicated in the insets).

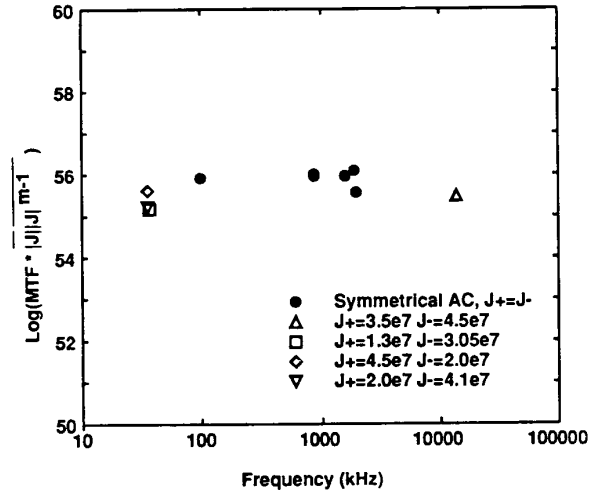


Fig.10. Plot of $A_{\text{AC}}(T)$ versus frequency for symmetrical and non-symmetrical waveforms. The data indicates that $A_{\text{AC}}(T)$ is insensitive to frequencies.

Upon examination of the failed test stripes under an optical microscope, it was noted that in almost all of the AC cases, the open failure sites in the short 100 μm stripes were found where the stripe joins the wider line (see Fig.11). This observation can be explained by speculation earlier that AC failures occur at sites where there is the largest non-symmetrical flow of vacancy flux. In this case, the imbalance of vacancy flux is caused by the geometry of the interconnect.

In each test group stressed using non-symmetrical AC waveforms, the open sites were preferentially located at the site that is the cathode side during the higher current half-cycles, i.e. if current from A to point B is higher than from B to A, the open site is at point B. We believe this is because the asymmetry of vacancy flux caused by the asymmetry of the test structure is reinforced by the asymmetry of the current waveform at this end of the stripe and counteracted at the other end. The failure sites of test stripes under symmetrical AC current stress were also preferentially, though to a lesser degree, located at one side of the bond pad, indicating a slight asymmetry of the current waveforms.

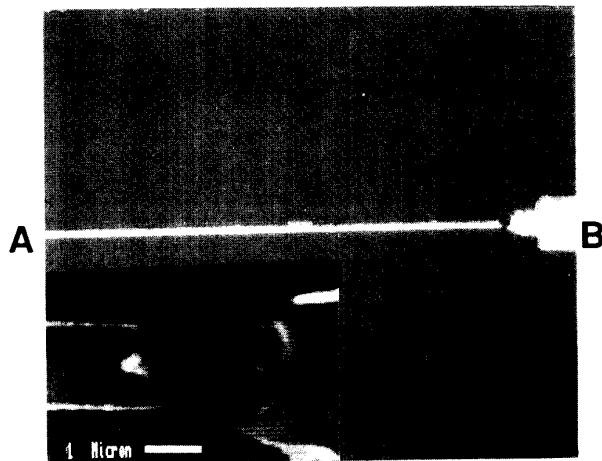


Fig.11. Photograph of failure site stressed with non-symmetrical pure AC waveform and a scanning electron micrograph of the failure site in the inset. The current density, J_+ from point A to B was $4.5 \times 10^7 \text{ A/cm}^2$ and J_- from point B to A was $2.0 \times 10^7 \text{ A/cm}^2$ during the other cycle. Open failure was preferentially located at B where the stripe joins the wider line because of the asymmetry of geometry, and the asymmetry of the current waveform.

Conclusions

We have shown that if constant DC current stress lifetime is proportional to J_m , the lifetime under pulse DC current stress, $\text{MTF}_{\text{pulse DC}}$ is inversely proportional to $\bar{J} \cdot J^{m-1}$. For the important special case of $m=2$, pulse DC stress lifetime is inversely proportional to the 2nd power of the time-averaged current density. For pure AC current stress, we have found that the AC lifetime of interconnect, MTF_{AC} , is typically much larger (~ 1000) than the DC lifetime because of the healing effect by the two opposing flow of vacancy flux. The magnitude of this enhancement factor for MTF_{AC} is insensitive to current densities, waveforms and frequencies that we have investigated but depends on the grain microstructure and the geometry of the interconnect. In our study, the latter effect seems to be the dominating factor in causing failure in short lines (100 μm) while the former dominates in longer (800 μm) lines. The pure AC lifetime for interconnect was shown to fit the Black's equation for DC electromigration failure, provided we replace J^m with $|\bar{J}| |J|^{m-1}$, and $A_{\text{DC}}(T)$ with $A_{\text{AC}}(T)$. We have found that the exponent m is the same in the DC (Eq.(7)) and AC electromigration equation (Eq.(15)).

Acknowledgement

This work was partially supported by ISTO/SDIO administered through ONR under Contract N00019-85-K-0603.

References

- [1] A. T. English and E. Kinsbron, "Electromigration transport mobility associated with pulsed direct current in fine-grained evaporated Al-0.5% Cu thin films," *J. Appl. Phys.*, vol. 54, p. 275, 1983.
- [2] R. J. Miller, "Electromigration failure under pulse test conditions," *Proc. 16th Ann. Rel. Phys. Symp. IEEE*, p. 241, 1978.
- [3] J. M. Towner and E. P. van de Ven, "Aluminum electromigration under pulsed d.c. conditions," *Proc. 21st Ann. Rel. Phys. Symp. IEEE*, p. 36, 1983.
- [4] L. Brooke, "Pulse current electromigration failure model," *Proc. 25th Ann. Rel. Phys. Symp. IEEE*, p. 136, 1987.
- [5] B. K. Liew, N. W. Cheung, and C. Hu, "Electromigration interconnect failure under pulse test conditions," *Proc. of the 1988 Symposium on VLSI Technology*, p. 59, 1988.
- [6] J. M. Schoen, "A model of electromigration failure under pulsed condition," *J. Appl. Phys.*, vol. 51, p. 508, 1980.
- [7] R. Shield and T. H. Ramsey, "Control of electromigration in aluminum interconnects," *Proc. 1969 Electron. Comp. Conf.*, p. 424, 1969.
- [8] J. C. Blair, P. B. Ghate and C. T. Haywood, "Electromigration-induced failures in aluminum film conductor," *Appl. Phys. Lett.*, vol. 19, p. 281, 1970.
- [9] A. J. Learn, "Effect of structure and processing on electromigration-induced failure in anodized aluminum," *J. Appl. Phys.*, vol. 44, p. 1251, 1973.